PAPER • OPEN ACCESS

Radial Fourier transforms in exoplanetary imaging and potential uses at Timau National Observatory

View the article online for updates and enhancements.

IOP ebooks™

Bringing you innovative digital publishing with leading voices to create your essential collection of books in STEM research.

Start exploring the collection - download the first chapter of every title for free.

Radial Fourier transforms in exoplanetary imaging and potential uses at Timau National Observatory

H Albanna[1,*], D Doelman[1] and F Mumtahana[2]

[1] Leiden Observatory, Leiden University, P.O. Box 9513, 2300 RA, Leiden, The Netherlands
[2] National Institute of Aeronautics and Space (LAPAN), Indonesia

Email: albanna@strw.leidenuniv.nl

Abstract. Due to Fourier transforms nature between the field detected on the image and its corresponding input, astronomical imaging can be modelled mathematically. In exoplanetary imaging, we aim to detect exoplanets whose typical contrast are approximately one over a million times dimmer compared to their parent stars. Among the possible approaches to accomplish that is optical apodization, a technique to purposely modify the input signal profile such that the 'Airy rings' on the resulting image are suppressed while keeping the central brightness high. In the paper, we pedagogically describe this technique applying Fourier transforms of radially-symmetric functions; and investigate potential future uses at Timau National Observatory.

*Keyword : Imaging, observatory, exoplanet, fourier transforms*

1. Introduction

The existence of worlds other than the earth has always been a great interest for humankind. Beginning from Galileo Galilei's observation of the phase of Venus in 1610, confirming that the planets orbit around the Sun, it then makes sense that other stars must also have companion planets. In fact, the discovery of exoplanets, planets around stars other than the Sun, has already started more than two decades ago. In 1992, Wolszczan and Frail detected the first exoplanet(s) orbiting not a solar-type star, but a pulsar [1]. They measured the timing of pulses of the pulsar which seemed to be irregular, indicating the existence of two planets. The first detection of an exoplanet around a Sun-like star follows not so long after, using radial velocity method. Mayor and Queloz observed a periodic variation on the radial velocity of 51 Pegasi. Another detection method is called transit method, first performed by Charbonneau *et al.*, which measures periodic dimming of the starlight during the planetary transit across the host star [2]. The exoplanet itself, HD 209458b, was already discovered with radial velocity method [3]. Other important methods are astrometry and microlensing, which makes use of the variation of the position of the star and the gravitational perturbation due to the foreground planet, respectively [4, 5, 6].

The techniques mentioned above are indirect methods to probe exoplanets. Together, those allow for determination of the exoplanet properties, such as period, radius, mass and temperature. For further characterization of the exoplanet, however, direct imaging is required. It gives ways to a more complete story than the indirect counterparts. Yet, it comes with several challenges, the biggest of which is the extremely dim flux of the planet, overwhelmed by the glare of its host star. To date, only 3 percent out of over 3500 exoplanet detections are detected directly, as shown in Figure 1. Only the largest telescopes and the most advanced techniques have been able to carry out such difficult tasks.

This paper is aimed to lessen those gaps, introducing a simple yet powerful principle behind exoplanetary imaging: optical apodization. Throughout the paper, we mostly use pedagogical approach in describing the technique; how and why it works, but we leave out the practical and/or manufacturing aspects, as those would require a different discussion and expertise.
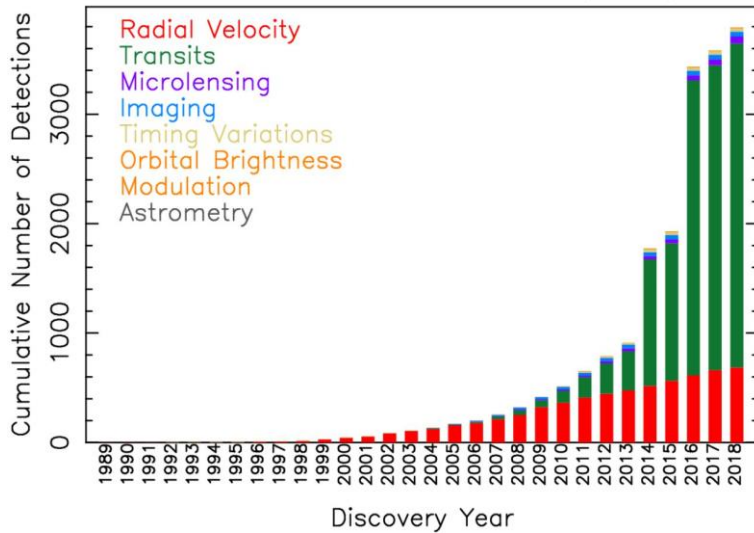
Figure 1. Cumulative number of exoplanet detections. Radial velocity and transits methods contribute the most with ~3600 detections combined. Direct imaging, being the most difficult technique, only shares less than 100 detections. Source: *https://exoplanetarchi ve.ipac.caltech.edu/*

2. Fourier transforms
2.1. Physical backgrounds
Using the Huygens-Fresnel principle which states that each point on a wave front can be regarded as a source of spherical secondary wavelets and the amplitude of the field at any point beyond is the superposition of these wavelets, one can arrive to the following result [7, 8, 9]

$$E(u,v) = \frac{e^{ik\left[z+\frac{u^2+v^2}{2z}\right]}}{i\lambda z} \iint_{-\infty}^{\infty} \tilde{E}(x,y)e^{-\frac{i2\pi(ux+vy)}{\lambda z}} dxdy, \tag{2.1}$$

where the field density, the aperture and the induced phase are embedded inside $\tilde{E}(x,y)$. This equation exactly resembles Fourier transform in two-dimension, with a multiplicative factor before the integral. Fixing $\lambda = z = 1$ to be unity and expressing the resulted lengths in terms of λ, the corresponding Fourier transform is then

$$F(u,v) = \iint_{-\infty}^{\infty} f(x,y)e^{-i2\pi(ux+vy)} dxdy. \tag{2.2}$$

After the normalization, the electric field pair $\tilde{E}(x,y) - E(u,v)$ and the Fourier transform pair $f(x,y) - F(u,v)$ are completely interchangeable, with (x,y) and (u,v) represent the coordinate systems in the pupil plane and the focal plane, respectively. In other words, from this point on it is possible to switch completely to mathematics without losing any physical meaning.

2.2. Fourier transforms in polar coordinates
Due to circular shape of telescope apertures, it is naturally more convenient to work in polar coordinate system instead of Cartesian. Moreover, when a function in the pupil plane has a circular symmetry, so does its resulting image, since they are related through Fourier transforms and Fourier transforms preserve the symmetry. If this is true, suppressing 360 degrees of starlight halo would also require patterns with circular symmetry, which suggests the use of polar coordinates. It will be more evident once the expressions are derived. Cartesian to polar coordinate system conversion is performed by introducing the following coordinates

$$x = r\cos\theta \, , \; y = r\sin\theta \, , \; u = \rho\cos\psi \, , \; v = \rho\sin\psi. \tag{2.3}$$

Substituting them into equation (2.2), we obtain

$$F(\rho, \psi) = \int_0^\infty \int_0^{2\pi} r f(r, \theta) e^{-i2\pi\rho r \cos(\theta - \psi)} \, dr d\theta \tag{2.4}$$

Any function $f(r, \theta)$ is always periodic in angular direction, so rewriting it in terms of Fourier series is possible

$$f(r, \theta) = \sum_{n=-\infty}^{\infty} a_n e^{i2\pi\left(\frac{n}{T}\right)\theta} \text{ with } a_n = \frac{1}{T} \int_{-\frac{T}{2}}^{\frac{T}{2}} f(r, \theta) \, e^{-i2\pi\left(\frac{n}{T}\right)\theta} \, d\theta, \tag{2.5}$$

to which we can plug a period of $T = 2\pi$, since it is periodic every full circle, and obtain

$$f(r, \theta) = \sum_{n=-\infty}^{\infty} f_n(r) e^{in\theta} \text{ with } f_n(r) = \frac{1}{2\pi} \int_{-\pi}^{\pi} f(r, \theta) \, e^{-in\theta} \, d\theta. \tag{2.6}$$

Hence, the overall Fourier transform becomes

$$F(\rho, \psi) = \sum_{n=-\infty}^{\infty} \int_0^\infty \int_0^{2\pi} r f_n(r) e^{in\theta - i2\pi\rho r \cos(\theta - \psi)} \, dr d\theta. \tag{2.7}$$

Part of the exponents can be expanded with the following relation which contains Bessel function of the first kind J_n of order n [10]

$$e^{-2\pi\vec{\rho}.\vec{r}} = e^{-2\pi\rho r \cos(\theta - \psi)} = \sum_{n=-\infty}^{\infty} (-i)^n 2\pi J_n(2\pi\rho r) e^{-in\theta} e^{in\psi}. \tag{2.8}$$

Plugging equation (2.8) into (2.7), we get the general expression of Fourier transforms in polar coordinates

$$F(\rho, \psi) = \sum_{n=-\infty}^{\infty} (-i)^n e^{in\psi} 2\pi \int_0^\infty r f_n(r) J_n(2\pi\rho r) \, dr, \tag{2.9}$$

where the azimuthal variation is stored in $f_n(r)$, taking the form

$$f_n(r) = \frac{1}{2\pi} \int_{-\pi}^{\pi} f(r, \theta) \, e^{-in\theta} \, d\theta. \tag{2.10}$$

If we examine the last two equations, it is made clear that the function $f(r, \theta)$ can consist of both radial and azimuthal modes. In this paper, we restrict ourselves only to the radial mode due to some considerations. First, working in radial mode would simplify the problem significantly. Removing angular mode in polar coordinates basically leaves one dimension to work with while keeping the two-dimensional shape. Second, Fourier transform symmetry-preserving nature suggests radially symmetric patterns for 360 degrees dark zone. However, when there is a need for further investigation in azimuthal functions, such as examining the effect of secondary mirror spiders, it is suggested to begin with equation (2.9) and (2.10).

2.3. Radial Fourier transforms
For radially symmetric functions, it is assumed that $f(r, \theta) = f(r)$ only depends on the radius. Hence, the Fourier series coefficients in equation (10) can be calculated as

$$f_n(r) = \frac{f(r)}{2\pi} \int_{-\pi}^{\pi} e^{-in\theta} \, d\theta = \frac{f(r)}{2\pi} \left[\frac{e^{-in\theta}}{-in} \right]_{-\pi}^{\pi} = \begin{cases} 0 & n \neq 0, \\ f(r) & n = 0. \end{cases} \tag{2.11}$$
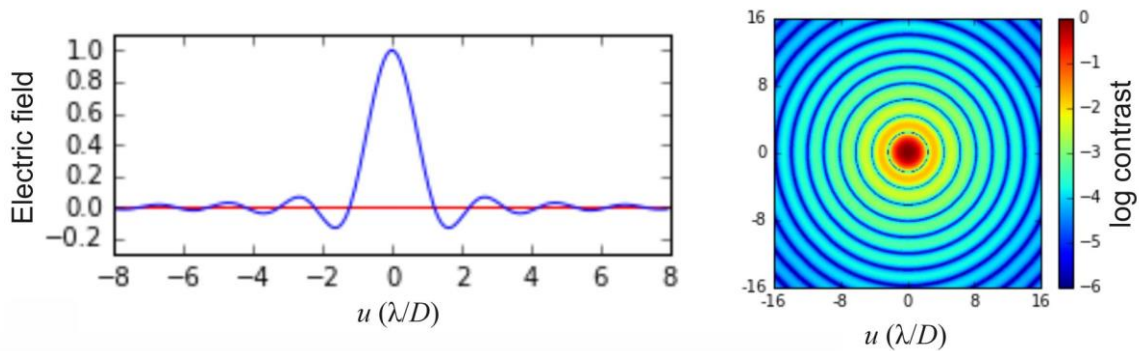
Figure 2. Airy function, a pattern resulted from a circular aperture. It closely resembles damped sinusoidal function. If there are more than one source, each source through the aperture would result in the same pattern with different amplitude based on its brightness.

This result significantly reduces the summation in equation (9) to only remains one non-zero term, which is for n = 0

$$F(\rho) = 2\pi \int_0^\infty r f(r) J_0(2\pi\rho r) dr. \tag{2.12}$$

The expression above makes it clearer that radial patterns at the pupil plane would surely generate radially symmetric structure at the focal plane. Hereafter, we refer Fourier transforms for radially symmetric functions as Radial Fourier Transforms (RFT).

3. Applying RFT

3.1. Apodization
Using equation (2.12), we can, for instance, calculate the image detected at the focal plane for a circular aperture by putting circular function

$$f(r) = \text{circ}\left(\frac{r}{a}\right) = \begin{cases} 1 & r < a, \\ 0 & r > a, \end{cases} \tag{3.1}$$

where a is the radius of the aperture. Then, making use of the following integral property of Bessel function

$$\int_0^\alpha x J_0(x) dx = \alpha J_1(\alpha), \tag{3.2}$$

we arrive at the historical Airy function

$$F(\rho) = a \frac{J_1(2\pi\rho a)}{\rho}. \tag{3.3}$$

The function is visually illustrated in Figure 3. Typical hot Jupiters would be located at around $2 - 5\lambda/D$, covered completely by the second or third Airy rings. This makes it extremely difficult to directly image exoplanets without any additional optical components. Two different kinds of modifications can be applied at the pupil plane: amplitude- and phase-apodization.[11][12] Both methods are principally similar, deciding the function $f(r)$ in equation (2.12)

$$f(r) = \begin{cases} A(r) & \text{amplitude-apodization,} \\ A(r).e^{i\phi(r)} & \text{phase-apodization.} \end{cases} \tag{3.4}$$
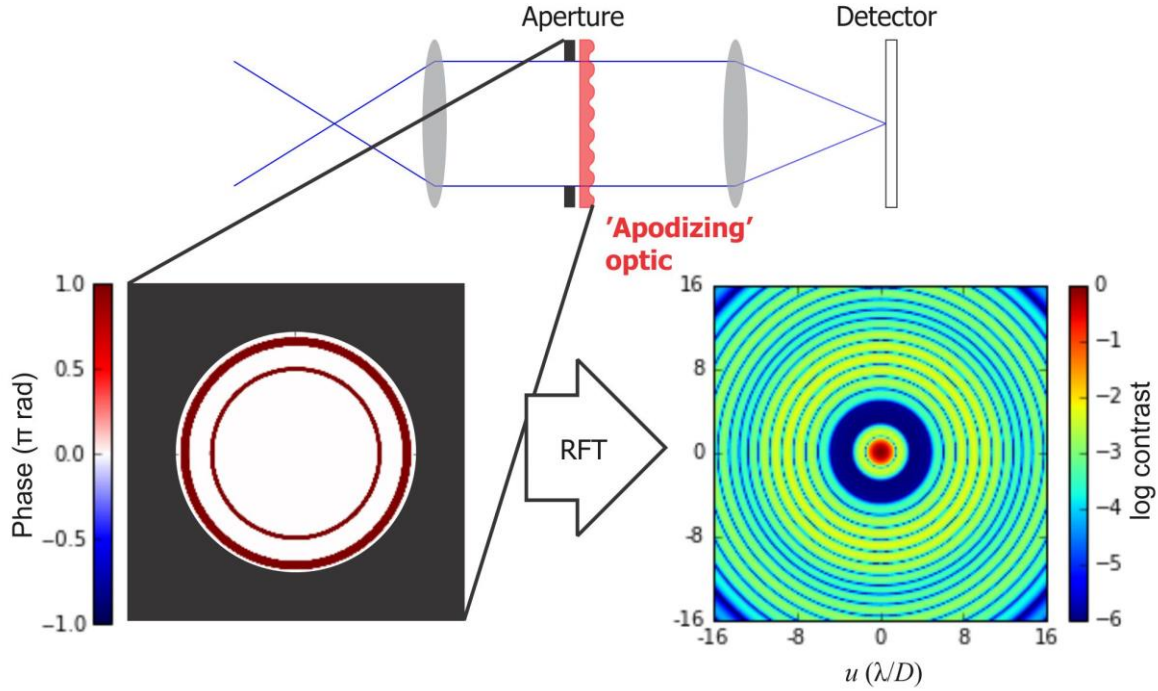
Figure 3. Configuration of phase-apodization principle. An 'apodizing' optic is applied at the pupil plane to form an extended dark region around the peak of the resulting image. At the bottom panel is a RFT pair of a working sample design of phase-apodizing coronagraph.

In amplitude-apodization, $A(r)$ consists of the original aperture shape and an amplitude mask to modify the signal; while in phase-apodization, $A(r)$ is the original aperture shape and $\phi(r)$ is a phase-inducing optics. The configuration is illustrated at the top panel of Figure 3. The first phase inducing-optics were made from ZnSe diamond-turned plates with varying height. Nowadays, devices to induce phases to liquid crystals have been created [13, 14]. Despite the different manufacturing methods, the desired outputs of those two methods are the same: suppressing the Airy rings within certain radius (hereafter working angle), while keeping the central brightness to be as high as possible. Mathematically, the first requirement translates to

$$\text{minimize} \left(\frac{1}{N} \sum_{i=0}^{N} \left| \frac{F_{\text{mod}}(\rho_i)}{F_{\text{mod}}(0)} \right|^2 - 10^{-6} \right), \tag{3.5}$$

with $N = (\rho_f - \rho_i)/\Delta\rho$ is the number of points to be evaluated and $\Delta\rho$ is small enough value. The assumed required contrast of 10^{-6} can be adapted accordingly. The *mod* subscripts stand for *modified*. Similarly, the second requirement translates to

$$\text{maximize} \left| \frac{F_{\text{mod}}(0)}{F_{\text{init}}(0)} \right|^2, \tag{3.6}$$

where *mod* represents the modified function with the mask/optic applied and *init* represents the initial function without one. These two requirements are generally sufficient to generate working coronagraph designs. In Figure 3, we present an example of phase-apodization with a working angle of $(\rho_i, \rho_f) = (3, 5) \, \lambda/D$.

3.2. Potential uses

There are at least three criteria to enable direct imaging of exoplanets: an extremely high contrast, a very high angular resolution, and a total field of view that includes the working angle.[15] Based on these criteria, we did a case study towards a future 3.8-meter optical telescope at Timau National Observatory, Indonesia,[16] coupled with a RFT-generated phase-apodizing coronagraph. With simulation, we managed to reach a high contrast of 10^{-6}; a typical exoplanet has a relative brightness of $10^{-5} - 10^{-10}$ compared to its parent star. For the angular resolution, we found a value of 0.04 arcsec at 700 nm, which can be considered to be high. Finally, an inner working angle of 3.1 λ/D from the simulation approximately coincides with 0.11 arcsec at 700 nm. As a reference, a 'twin Jupiter' at 10 pc from us would have a separation of 0.5 arcsec, which would be within our simulated working angle. We positively conclude that the configuration can potentially detect exoplanets directly.

4. Conclusion

The basic principle behind one of exoplanetary imaging methods, optical apodization, has been discussed, starting from Huygens-Fresnel principle to a specific application of Fourier transforms for radially symmetric functions. With this technique, the future 3.8-meter telescope at Timau National Observatory should be able to directly image Jupiter-sized exoplanets at 10 pc distance.

Acknowledgements

References

[1]   Wolszczan A and Frail D A 1992 *Nature* **355.6356** p 145
[2]   Mayor M and Queloz D 1995 *Nature* **378.6555** p 355
[3]   Charbonneau D *et al* 1999 *Astrophys. J. Lett.* **529.1** p L45
[4]   Mazeh T *et al* 2000 *Astrophys. J. Lett.* **532.1** p L55
[5]   Perryman M *et al* 2014 *Astrophys. J.* **797.1** p 14
[6]   Gaudi B S 2012 *Annu. Rev. Astron. Astrophys.* **50** pp 411–453
[7]   Huygens C 2012 *Treatise on Light* tredition
[8]   Goodman J W 1996 *Introduction to Fourier Optics* McGraw-Hill Book Co New York
[9]   Hecht E 1998 *Optics 4th edition* Addison Wesley Longman Inc
[10]   Kyatkin A B and Chirikjian G S 2000 *Engineering Applications of Noncommutative Harmonic Analysis: with Emphasis on Rotation and Motion Groups* CRC press
[11]   Codona J L *et al* 2006 *Proc. SPIE* **6269** 62691N
[12]   Kenworthy M A *et al* 2007 *Astrophys. J.* **660.1** p 762
[13]   Snik *et al* 2012 *SPIE* **8450** p 84500M
[14]   Otten G P *et al* 2014 *SPIE* **9151** p 91511R
[15]   Burrows A 2005 *Nature* **433** pp 261–268
[16]   Mumpuni E S *et al* 2017 *Selayang Pandang Observatorium Nasional Timau* PT Gramedia Jakarta